

Lawrence Berkeley National Laboratory

LBL Publications

Title

Baseflow Age Distributions and Depth of Active Groundwater Flow in a Snow-Dominated Mountain Headwater Basin

Permalink

<https://escholarship.org/uc/item/3sb9g0wm>

Journal

Water Resources Research, 56(12)

ISSN

0043-1397

Authors

Carroll, Rosemary WH
Manning, Andrew H
Niswonger, Richard
[et al.](#)

Publication Date

2020-12-01

DOI

10.1029/2020wr028161

Peer reviewed

Water Resources Research



RESEARCH ARTICLE

10.1029/2020WR028161

Key Points:

- Gas tracer data in baseflow that indicate deeper flows through bedrock are an important source to steep, mountain streams
- Historical variability in baseflow age (3–12 years) is dictated by interflow with groundwater contributions stable (11.8 ± 0.7 years)
- Precipitation defines groundwater age sensitivity with flow paths getting deeper and older in a slightly drier future

Supporting Information:

- Supporting Information S1

Correspondence to:

R. W. H. Carroll,
rosemary.carroll@dri.edu

Citation:






Carroll, R. W. H., Manning, A. H., Niswonger, R., Marchetti, D., & Williams, K. H. (2020). Baseflow age distributions and depth of active groundwater flow in a snow-dominated mountain headwater basin. *Water Resources Research*, 56, e2020WR028161. <https://doi.org/10.1029/2020WR028161>

Received 15 JUN 2020

Accepted 8 NOV 2020

Accepted article online 18 NOV 2020

Baseflow Age Distributions and Depth of Active Groundwater Flow in a Snow-Dominated Mountain Headwater Basin

Rosemary W. H. Carroll¹ , Andrew H. Manning² , Richard Niswonger³ , David Marchetti⁴ , and Kenneth H. Williams^{5,6} 

¹Desert Research Institute, Reno, NV, USA, ²U.S. Geological Survey, Denver, CO, USA, ³U.S. Geological Survey, Menlo Park, CA, USA, ⁴Natural and Environmental Sciences (NES) Department, Western Colorado University, Gunnison, CO, USA, ⁵Lawrence Berkeley National Laboratory, Berkeley, CA, USA, ⁶Rocky Mountain Biological Laboratory, Gothic, CO, USA

Abstract Deeper flows through bedrock in mountain watersheds could be important, but lack of data to characterize bedrock properties limits understanding. To address data scarcity, we combine a previously published integrated hydrologic model of a snow-dominated, headwater basin of the Colorado River with a new method for dating baseflow age using dissolved gas tracers SF₆, CFC-113, N₂, and Ar. The original flow model predicts the majority of groundwater flow through shallow alluvium (<8 m) sitting on top of less permeable bedrock. The water moves too quickly and is unable to reproduce observed SF₆ concentrations. To match gas data, bedrock permeability is increased to allow a larger fraction of deeper and older groundwater flow (median 112 m). The updated hydrologic model indicates interannual variability in baseflow age (3–12 years) is controlled by the volume of seasonal interflow and tightly coupled to snow accumulation and monsoon rain. Deeper groundwater flow remains stable (11.7 ± 0.7 years) as a function mean historical recharge to bedrock hydraulic conductivity (R/K). A sensitivity analysis suggests that increasing bedrock K effectively moves this alpine basin away from its original conceptualization of hyperlocalized groundwater flow (high R/K) with groundwater age insensitive to changes in water inputs. Instead, this basin is situated close to the precipitation threshold defining recharge controlled groundwater flow conditions (low R/K) in which groundwater age increases with small reductions in precipitation. Work stresses the need to explore alternative methods characterizing bedrock properties in mountain basins to better quantify deeper groundwater flow and predict their hydrologic response to change.

Plain Language Summary Snow in mountain systems is an important water source but little is understood how snow processes dictate groundwater flow paths, the age of stream water, and its sensitivity to climate or land use change. We use a recently developed stream water gas tracer experiment in a steep mountain stream in a Colorado River headwater basin. A hydrologic model cannot match gas tracer data if groundwater flow is shallow, moving through the unconsolidated material near land surface, because groundwater moves too quickly. Instead, groundwater must follow deeper, longer flow paths through the fractured granitic bedrock. A sensitivity analysis shows that this snow-dominated headwater basin is functioning near a precipitation threshold. With wetter conditions, little change occurs to groundwater flow paths and ages are insensitive to changes in climate or forest removal. However, with small decreases in snowpack accumulation, groundwater flow paths become increasingly deeper and older. Collecting stream water gas data helped identify groundwater flow path sensitivity to climate and land use change.

1. Introduction

Baseflow represents stream water derived from both shallow and deep subsurface flow paths that sustain late summer streamflow after precipitation or snowmelt events cease. Baseflow is recognized as an important source to stream water in mountainous watersheds (Gabielli et al., 2012; Hale & McDonnell, 2016; Miller et al., 2016; Rumsey et al., 2015). It reflects the integrated effects of surface processes controlling hydrologic partitioning of rain and snowmelt to evapotranspiration (ET) and subsurface flow, as well as the distribution of subsurface permeability and the relative importance of groundwater circulating to different depths. *Interflow* or shallow, ephemeral flow through the soil (and saprolite) occurs through either

©2020. The Authors.

This is an open access article under the terms of the Creative Commons Attribution License, which permits use, distribution and reproduction in any medium, provided the original work is properly cited.

strong permeability contrasts or a seasonally rising water table. Interflow reaches a stream network on the order of days to weeks. In contrast, saturated *groundwater* moving through alluvial and bedrock units can have a wide range of flow paths and travel times reflect lithology, fracture networks, and geologic structure (Heidbüchel et al., 2012). Groundwater contributions to streams are important for the biologic integrity of the river network (Meyer et al., 2007; Missik et al., 2019), while the time water spends in the subsurface interacting with host material directly influences biogeochemical processes that control mineral weathering (Winnick et al., 2017) and carbon dynamics (Brooks et al., 2015; Perdrial et al., 2018). Subsurface residence time also indicates the degree of catchment memory of past inputs to reflect hydrologic sensitivity to land use and climate change (McGuire et al., 2005) and potential persistence of contamination (Mahlknecht et al., 2017).

There is a growing recognition that deeper parts of bedrock aquifers in mountain watersheds could be an important component of the hydrologic system (Condon et al., 2020), transmitting and storing a larger amount of water and having a larger influence on stream biogeochemical processes than previously appreciated. However, the codependant relationships between climate, topography, and vegetation in mountain watersheds and their interactions with subsurface geology to affect depth of subsurface flow paths and resultant stream water age distributions remains poorly understood. This is largely due to a lack of data characterizing watershed-scale heterogeneity of snow distribution and melt dynamics (Deems et al., 2006; Harpold et al., 2012), soil water storage and losses to ET (Allen et al., 2013; Wang & Dickinson, 2012), subsurface hydraulic properties (Meixner et al., 2016), and active circulation depths (Frisbee et al., 2016).

Lumped parameter approaches have been applied to numerous catchments lacking detailed hydrologic characterization (McGuire & McDonnell, 2006). The age of streamflow (or catchment transit time) is estimated by the convolution of time-varying inputs of an environmental tracer (e.g., ^3H , $\delta^2\text{H}$, $\delta^{18}\text{O}$, and Cl) applied uniformly across a watershed and lagged through the subsurface by assuming a travel time distribution (e.g., piston flow [PF], exponential, gamma, Weibull, and dispersion) that is adjusted to match observed tracer concentrations in streamflow. Recently, lumped-parameter approaches have been developed that include variance in travel time distributions to address seasonal changes in flow pathways and mobilization of stored water of varying age (Botter et al., 2011; Harman, 2015; van der Velde et al., 2012). These analytical solutions have been applied to a variety of scenarios, including the influence of snow processes on streamflow (Fang et al., 2019) and selective vegetation uptake (Smith et al., 2018). In contrast to these low-order modeling strategies, numerical mechanistic models and particle tracking can include complex boundary conditions and directly represent physical and hydrological characteristics dictating catchment flow pathways that determine the travel time distribution (Danesh-Yazdi et al., 2018; Engdahl et al., 2016; Maxwell et al., 2016). These models provide a powerful platform to study basin sensitivity to changing climate and other conditions, but their application in steep, mountainous basins is still limited by data scarcity, with bedrock hydrologic data on permeability, porosity, and flow rates extremely rare. Data that do exist are complicated by the difficulty in characterizing fractured bedrock (Cesano et al., 2003) that are typically dominant in mountain basins. Lack of subsurface data in mountain systems makes quantifying groundwater flow at depth and its relative importance in mountain hydrology uncertain. This knowledge gap remains a major impediment to properly incorporating the deeper subsurface flow system into hydrologic models of mountainous watersheds and assessing the relative importance of groundwater on stream water exports.

To address data scarcity inherent to mountain systems, we apply a method for dating baseflow presented by Sanford et al. (2015) using stream water N_2 , Ar, SF_6 , and CFC-113 observations collected over a 12-hr period in Copper Creek, Colorado (24 km^2), a snow-dominated, headwater basin of the Colorado River. The method's effectiveness for describing a unique streamflow age distribution has been demonstrated in low-to-moderate-gradient streams but has not been applied in a high-gradient system where it could be hampered by fast gas exchange velocities to the atmosphere (Gleeson et al., 2018; Solomon et al., 1998). This study seeks to validate the gas tracer methodology in a high gradient stream and use the baseflow age information as an indirect observation of subsurface properties within a previously published hydrologic model of the basin (Carroll et al., 2019). The second objective is to use the gas tracer informed hydrologic model to explore the relative importance of shallow versus deeper subsurface flow contributions to stream water as a function of baseflow age. Lastly, we explore sensitivity of groundwater flow paths to changes in climate and land use.

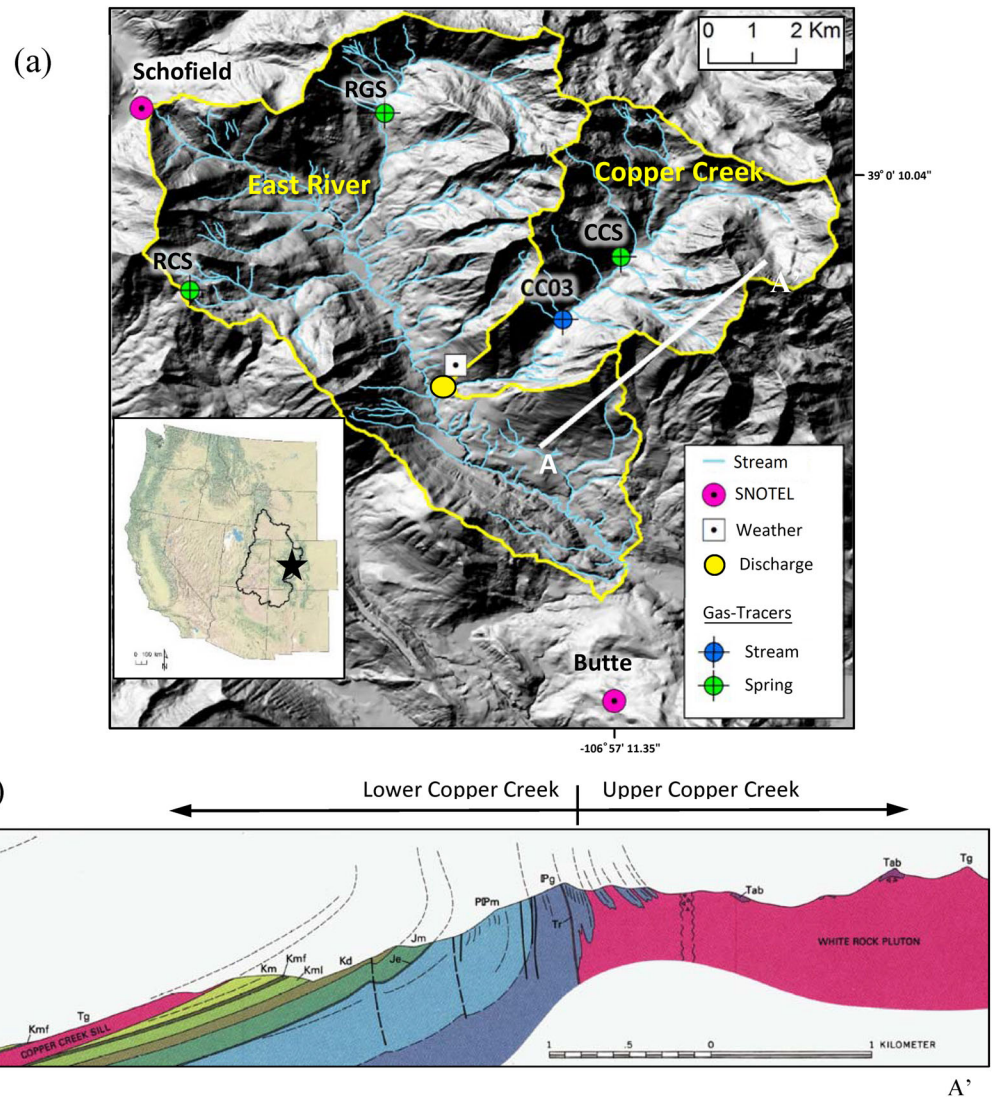


Figure 1. (a) The East River with Copper Creek delineated. Inset shows location of the site in the context of the western United States and the Upper Colorado River Basin. (b) Geologic cross-section A-A' modified from (Gaskill et al., 1991) with geologic units described in Table 1.

2. Site Description

The East River (85 km²) is a seasonally snow covered, mountainous watershed in the headwaters of the Upper Colorado River (Figure 1) located near Crested Butte, Colorado. A comprehensive overview of the site is provided by Carroll et al. (2018) and Hubbard et al. (2018). Climate is continental subarctic, and stream discharge is dominated by snowmelt with peak flows occurring in early June and receding through the summer and fall. Monsoon rains occur in the summer months. This study is focused on Copper Creek (24 km²), the largest tributary of the East River. Land cover is predominantly barren alpine (50%) and conifer forests (36%) with smaller representations of meadows, shrubs, and aspen. Elevations range from 2,880 to 4,128 m. The upper portion of the watershed and adjacent peaks is underlain by Tertiary granodiorite. This younger, intrusive rock has upturned Paleozoic and Mesozoic sedimentary strata into steeply dipping hydrostratigraphic units that underlay the lower portion of Copper Creek (Figure 1b). Talus, rock glaciers, and alluvial fans dominate surficial deposits within Copper Creek's glacially sculpted valleys (Gaskill et al., 1991). Descriptions of individual geologic units are provided in Table 1.

Table 1
Geologic Units in Copper Creek (Modified From Gaskill et al., 1991) and Model-Specified Parameters

Unit	Epoch	Name	Description (modified Gaskill et al., 1991)	K0 (m/s) ^a	VKA ^b	Surface porosity ^c	Deep porosity ^d
Qal	Holocene	Surface deposits	Alluvium, fans, debris flow, landslide, talus, rock glaciers	1.2×10^{-5} 1.1×10^{-4}	1	0.2	0.1
Tg	Oligocene	Granodiorite	White Rock Pluton—quartz diorite to quartz manzonite	4.6×10^{-7}	3	0.036	0.018
Sill	Oligocene	Granodiorite	Quartz diorite to quartz manzonite	4.6×10^{-7}	3	0.036	0.018
Km ¹	Upper Cretaceous	Main body	Mostly silty to sandy marine shale	1.2×10^{-6}	3	0.1	0.05
		Mancos Shale					
Km ²	Upper Cretaceous	Lower member	Interbedded silty and sandy, calcareous marine shale, siltstone	1.2×10^{-6}	3	0.1	0.05
		Mancos Shale					
Kd	Upper Cretaceous	Dakota sandstone	Quartzitic sandstone grading upward to carbonaceous shale, sandstone, siltstone to fine grained quartzite	5.8×10^{-6}	3	0.1	0.05
JmJe	Upper/Middle Jurassic	Morrison Fm (Jm) & Entrada sandstone (Je)	Jm: claystone, siltstone, and shale (65%) interlensed with cherty sandstone (30%). Je: thick bedded, cross-laminated quartz-arenite, or quartzite	1.2×10^{-6}	3	0.1	0.05
PPm	Lower Permian/Upper-Middle Pennsylvanian	Maroon Fm	Siltstone and sandstone interbedded with conglomerate, mudstone, and limestone	5.8×10^{-6}	3	0.1	0.05
Pg	Middle Pennsylvanian	Gothic Fm	Interbedded sandstone, limestone, siltstone, shale, and conglomerate. Metamorphosed along igneous contact	1.2×10^{-6}	3	0.1	0.05

^aSurface hydraulic conductivity (K0) in Layer 1. Hydraulic conductivity (K) declines exponentially with depth below ground surface (x). $K = K0e^{-0004x}$. ^bRatio of vertical to horizontal hydraulic conductivity (anisotropy). ^cSurface applies to model Layers 1 and 2 (≤ 18 m). ^dDeep applies to model Layers 3–12 (18–400 m).

Original hydrological modeling of Copper Creek for years 1987–2018 captures a wide range of snow accumulation and snowmelt scenarios and estimates annual precipitation equal to 1.39 ± 0.27 m/year, of which $78 \pm 7\%$ is snow (mean \pm sd; see section 3.2 for a description of method) (Carroll et al., 2019). Annually, the basin is simulated as energy limited (potential ET < precipitation) with average ET losses equal to 36% of annual precipitation. The model indicates that the bulk of ET is lost from the soil zone (67% ET), and lesser amounts are lost from sublimation (13% ET), canopy evaporation (9% ET), and groundwater ET (11% ET). On average, stream water is estimated 65% interflow and 35% groundwater, with groundwater volumetric contributions to streamflow relatively stable across the historical period.

3. Methods

3.1. Atmospheric Gas Tracers

3.1.1. Sample Collection and Analysis

Stream water dissolved gas samples were collected following the approach presented by Sanford et al. (2015). Samples were collected hourly for two relatively inert atmospheric gases (N₂ and Ar) and two gas age tracers (SF₆ and CFC-113) over a 12-hr period. The stream sampling site, CC03 (Figure 1), was chosen because it is located low in the watershed, allowing an integrated baseflow age estimate representing most of Copper Creek but is above a steep canyon containing large waterfalls to minimize degassing. The stream section immediately upstream of the site was free of deep pools and zones of anomalously high turbulence. The location is 2 km above the confluence of Copper Creek to the East River and resides just below the geologic interface between the upper basin bedrock of granodiorite and the lower basin sedimentary strata of higher permeability. The experiment was conducted on 27 August 2017, which is late enough in the year to potentially avoid monsoon rains and possible surface runoff contributions to the stream yet early enough to still have large diurnal stream temperature fluctuations characteristic of summer months. Stream water temperature was measured every 5 min (Solinst Level Logger Edge M3001 LT F6/M2) beginning the day

before and extending through the gas sampling period. Local barometric pressure was obtained from a Rocky Mountain Biological Laboratory weather station located 1.9 km from CC03 (Figure 1) and adjusted for the elevational difference of 70 m. Water samples for N₂, Ar, SF₆, and CFC-113 were collected in duplicate every hour from 8:30 a.m. to 8:30 p.m. (supporting information Tables S1 and S2), to capture minimum and maximum diurnal stream fluctuation. Samples were collected using a peristaltic pump and polyethylene tubing placed several centimeters off the stream bed (stream depth 0.3 m). Sample containers were filled using techniques described at the U.S. Geological Survey's (USGS) Reston Groundwater Dating Laboratory website (USGS, 2017), stored on ice, and shipped the next day to the USGS Dating Laboratory for analysis. Samples for CFC-113 and SF₆ were analyzed using purge and trap gas chromatography with an electron capture detector (GC-ECD), while samples for N₂ and Ar were analyzed using gas chromatography with a thermal conductivity detector (GC-TCD, USGS, 2017). Measurement errors based on the sample duplicates were 1.7% for N₂, 1.4% for Ar, and 1% for SF₆ and CFC-113, these being consistent with lab-reported errors (USGS, 2017).

Dissolved SF₆ concentrations were measured in three perennial springs located in the vicinity of CC03 to provide independent groundwater age information (Figure 1). Samples were collected in July and October 2017. Argon and N₂ were measured in two of these springs. Spring CCS is located higher in the Copper Creek watershed 1.7 km from CC03, and springs RCS and RGS are located within adjacent tributaries of the East River 5.4 and 6.7 km from CC03, respectively. All three springs are at elevations between 3,200 to 3,500 m. Dissolved gases were collected using a peristaltic pump with the intake attached to a PushPoint pore water sampler (PPX36, <https://www.mheproducts.com/>) inserted into the shallow sediment at the bottom of each spring pool. Sample collection followed the same protocols indicated above (USGS, 2017), and all samples were analyzed by the USGS Dating Lab.

3.1.2. Tracer Data Interpretation

Following Sanford et al. (2015), measured stream dissolved gas concentrations were used with stream temperature and local atmospheric pressure measurements to simultaneously solve for the rates of gas and water exchange into and out of the stream, as well as the concentration of the gases in groundwater discharging into the stream. A control volume approach accounts for all inputs and outputs of water and gas along the length of the stream and assumes gases are nonreactive. The change in gas concentration in the stream (C_s [M/L³]) with time [t] was described by the following mass balance equation (Equation 11 in Sanford et al., 2015):

$$\frac{dC_s}{dt} = \frac{1}{\tau_w}(C_{gw} - C_s) - \frac{1}{\tau_g}(C_s - C_e), \quad (1)$$

where C_{gw} (M/L³) is the gas concentration in groundwater discharging into the stream; C_e (M/L³) is the atmospheric equilibrium gas concentration; τ_w (t) is the water residence time in the stream, equal to the stream depth divided by the rate of upward groundwater seepage through the streambed; and τ_g (t) is the gas residence time in the stream, equal to the stream water depth divided by the gas transfer velocity (v_g [L/t]). The gas transfer velocity governs the rate of gas exchange between the stream and the atmosphere. Stream concentrations are an intermediate value between C_{gw} and C_e ; if $\tau_w \ll \tau_g$, then C_s approaches C_{gw} , and if $\tau_w \gg \tau_g$, then C_s approaches C_e and it is difficult to discern C_{gw} .

The equilibrium gas concentration fluctuates due to diurnal stream temperature oscillations and can be computed using Henry's Law with the form:

$$C_e = P_a e^a + b \left(\frac{100}{T} \right) + c \ln \left(\frac{T}{100} \right) + d \left(\frac{T}{100} \right), \quad (2)$$

where P_a is the dry atmospheric pressure (atm), T is the stream temperature (Kelvin), and a , b , c , and d are gas-specific coefficients. The method takes advantage of the oscillatory variation of C_e with time to simultaneously solve for C_{gw} , τ_w , and τ_g for each gas using an explicit finite difference representation of Equation 1. Because τ_g is one of the computed parameters, a key advantage of this method, over many other techniques using dissolved gas tracers in streams to characterize groundwater inputs, is that it does not require an independent determination of v_g . The purpose of measuring concentrations of N₂ and Ar, in addition to the age tracer gases, is that they can estimate the recharge temperature (T_r) and excess air

concentration (A_e , [M/L³]) for groundwater. The recharge temperature is the temperature at the water table at the recharge location, and A_e is an excess component of air dissolved in groundwater due to the dissolution of air bubbles trapped when the water table rises during recharge events (Stute & Schlosser, 2000). The unfractionated air model of excess air formation (Aeschbach-Hertig et al., 2000) was assumed in this study. When T_r and A_e were known, estimated values of C_{gw} for SF₆ and CFC-113 were used to calculate their atmospheric concentrations at the time of recharge, which in turn provides a mean age for baseflow through use of an assumed travel time distribution (Busenberg & Plummer, 2002). Sanford et al. (2015) assumed a Weibull distribution in which the cumulative distribution function (CDF) is defined as follows:

$$CDF = 1 - e^{-(kt)^n}, \quad (3)$$

in which the scale parameter (k) and shape parameter (n) are adjusted to match the computed atmospheric concentration to the historical record (USGS, 2017). The Weibull distribution is equivalent to the exponential mixing model when $n = 1$.

Values of C_{gw} for each gas were estimated using a modified version of the Excel spreadsheet calculator developed by Sanford et al. (2015), which minimizes the misfit between measured and modeled values of C_s employing the automated General Reduced Gradient solver tool (provided as supporting documentation). Modifications included a reduced time step from 0.25 to 0.1 hr and expressing the misfit between measured and modeled values with the sum chi-square (χ^2), rather the sum squared error, to assess statistical significance of predicted water column concentrations. The sum χ^2 is the square of the difference in measured and modeled values divided by the square of the measurement error. Following Sanford et al. (2015), up to nine parameters can be adjusted to match stream gas concentrations: T_r , A_e , groundwater excess N₂ (potentially present from denitrification), τ_w , a single gas residence time for N₂ and Ar, gas residence times for SF₆ and CFC-113, and C_{gw} values for SF₆ and CFC-113.

For springs CCS and RCS, T_r and A_e values were derived from measured N₂ and Ar concentrations and used to compute a PF groundwater age from the measured SF₆ concentration using standard methods (USGS, 2017). The PF model (uniform sample age) was assumed instead of a more realistic age distribution (mixed-age sample) because the purpose of the spring samples was to provide a reasonable estimate of expected groundwater ages for the watershed, and the PF age likely differs little from the actual sample mean age for samples as young as these springs (e.g., <3 years difference assuming an exponential model for samples <15 years old). The recharge elevation was assumed to be the approximate mean elevation of the portion of the watershed directly upslope of the sampled spring. For spring RGS, Ar and N₂ were not collected and the mean T_r and A_e from the other two springs was used in the calculation of the PF age.

3.2. Integrated Hydrologic Model

Simulated energy and water budget components in Copper Creek rely on the USGS Groundwater and Surface water Flow model (GSFLOW, Markstrom et al., 2008). GSFLOW dynamically couples the USGS Precipitation-Runoff Modeling System (PRMS, Markstrom et al., 2015) and the Newton formulation of the USGS 3-D Modular Groundwater Flow model (Harbaugh, 2005; Niswonger et al., 2011) and 1-D simplification of Richard's equation for the unsaturated zone (Niswonger et al., 2006). The model describes daily surface and groundwater interactions related to ET including soil evaporation and plant transpiration, canopy interception, snow sublimation, and groundwater ET. The hydrologic model also estimates interflow, groundwater recharge, change in groundwater storage, and groundwater-surface water exchanges derived from differential gradients between groundwater and stream water elevations (Huntington & Niswonger, 2012) and deeper groundwater flow based on lithology and geologic structure.

Hydrologic model parameterization was based on the approach of Carroll et al. (2019). The finite difference grid resolution was 100 m with elevations resampled from the USGS National Elevation Dataset. Landfire (2015) was used to derive parameters of dominant cover type (Figure S5b), summer and winter cover density, canopy interception characteristics for snow and rain, and transmission coefficients for short-wave solar radiation. Climate forcing for water years 1987–2018 uses minimum and maximum daily temperature lapse rates defined by the two proximal Snow Telemetry (SNOTEL, Figure 1) stations adjusted for aspect. Scofield SNOTEL precipitation was spatially distributed using LiDAR-derived snow depth

observations from the Airborne Snow Observatory (ASO, Painter et al., 2016) during peak snow accumulation on an average water year (4 April 2016, Figure S5a) and adjusted for simulated losses associated with sublimation, canopy interception, and early melt prior to the flight.

Maximum soil water storage was conceptualized as a field capacity threshold above which water is partitioned to either lateral interflow or allowed to percolate downward via gravity drainage into the unsaturated zone (recharge). The spatial distribution of maximum soil storage was the product of rooting depth obtained from Landfire (2015) and available water content as a function of soil type (NRCS, 1991). The Copper Creek geologic model (Figure S5c) contains nine hydrostratigraphic units with 12 layers ranging in thickness from 8 to 120 m for a total thickness of 400 m. Fracture networks were not simulated. Instead, we used effective hydraulic conductivity that decreased exponentially with depth. The decay coefficient was established as a compromise between isotropic conditions and a fully localized flow system (Jiang et al., 2009), while the surface hydraulic conductivity was optimized to match average observed baseflow at the stream gauge located at the terminus of the basin.

3.2.1. Simulated Baseflow Age Distribution

Baseflow was simulated as the sum of saturated groundwater flow through alluvial and bedrock units and seasonal, shallow interflow. These two components were handled separately because GSFLOW only produces a velocity field for the groundwater system. To accommodate this limitation, GSFLOW was run fully coupled to generate interflow and all fluxes into and out of the groundwater system as well as the resulting water table elevations. Groundwater fluxes included recharge from water seepage below the soil zone plus ephemeral stream leakage, and groundwater ET losses back to the atmosphere. The groundwater model was then decoupled from GSFLOW, and particles (Mpath7; Pollock, 2016) were draped onto the water table surface and run forward in time using GSFLOW generated fluxes. Following Gusyev et al. (2014), individual flow path ages were weighted by calculated recharge but were also corrected by removing the volume-weighted age distribution of groundwater ET determined with backward particle tracking. Particle tracking established the groundwater age CDF delivered to the stream. Lastly, the volume of late August interflow was assumed to be less than 1 year old and added to groundwater age distribution to establish the baseflow age CDF.

Simulated baseflow age distributions test the hydrologic model's ability to reproduce the observed gas tracer water column concentrations at the end of August 2017. Initial water table elevations and water fluxes for water year 2017 initiated the particle tracking simulation followed by historical climate conditions for 1987 to 2018 repeated until all particles exit the watershed. A Weibull distribution (k and n , Equation 3) was adjusted to the flow model baseflow age distribution to solve for stream water SF₆ water column concentrations using Equation 1. The approach was Sanford et al. (2015) in reverse. The calculation of SF₆ water column concentrations required tracer-based estimates of A_e and T_r , an assumed recharge elevation of 3,400 m (the approximate mean elevation of the watershed above CC03) and the historical atmospheric concentration record (USGS, 2017). If the age distribution was unable to replicate observed stream concentrations based on the sum χ^2 , then subsurface porosity was adjusted to modify water velocities while avoiding any change to the original hydraulic gradients. If adjusting porosity was insufficient to create a statistically significant reproduction of observed gas tracers, then recalibration of the hydrologic model was considered. Recalibration focuses on alluvial and bedrock parameterization based on groundwater age sensitivities (refer to supporting information S2) and not the partitioning between interflow and recharge. The amount of interflow was largely dictated by the maximum soil storage, and it is constrained by observed streamflow during spring snowmelt. However, there is a feedback between groundwater parameterization and interflow such that if water table elevations rise into the soil zone then interflow was generated. If water table elevations are changed through reparameterization of the groundwater system, then some adjustment to the soil system may need to occur to match observed spring runoff. Using the recalibrated model, additional transient simulations explored interannual variability in baseflow age distributions across a range in historical climate conditions. These years include an extremely wet year (1995), a dry year at the end of a multiyear drought (2002), a dry year with a high-precipitation monsoon (2012), a dry year with a low-precipitation monsoon (2018), and the median water year (1998).

Steady-state particle tracking provided information on how deeper groundwater flow paths may change by shifting the historical mean groundwater condition as a function of altering precipitation, temperature, and forest presence. The historical median snow accumulation water year (1998) was used as a baseline

condition from which precipitation was incrementally adjusted by 0.4 to 1.8 of the historical daily value with no warming (+0°C). These conditions were repeated for +4°C and +10°C warming applied to both minimum and maximum daily temperatures. The +4°C condition falls in the range of expected end-of-century temperature increase in the East River (Hay et al., 2011), while +10°C forced all snow to fall as rain. Historical years were also run to steady state to explore variable precipitation type and timing on groundwater age distributions, while the effects of the spatial distribution of precipitation and temperature were tested by assigning uniform daily values. This removed gradients associated with elevation, storm tracking, and snow redistribution. Lastly, the relative importance of forest influences on energy and water budget partitioning and baseflow age was explored by removing deciduous and conifer forests from the basin. Forests were replaced by a barren cover type and the reparameterization of transmission coefficients for shortwave radiation, interception of precipitation, and rooting depths. Maximum soil storage and its conductance were not altered. Hypothetical scenarios were not representative of possible future conditions but a means to explore thresholds in groundwater flow paths as a function of climate and land use. For each scenario, daily climate for a complete water year was repeated until quasi-steady-state conditions occurred. Quasi-steady state was complete when combined changes in saturated and unsaturated groundwater storage were less than 1% the annual water budget. Cell-specific groundwater fluxes (recharge, ephemeral stream losses, and groundwater ET) were aggregated to an annual sum and applied to the water table surface of the steady state, decoupled groundwater model for particle tracking.

4. Results

4.1. Atmospheric Gas Tracers

Measured N_2 , Ar, and SF_6 concentrations along with computed T_r , A_e , and PF ages for the three sampled springs are shown in Tables S3 and S4. PF ages ranged from 3 to 14 years. The samples from CCS were collected in June after large snowpack accumulation and had the youngest ages (3 to 6 years). The younger ages and warm mean T_r of 9.2°C (near the top of the expected range of 0–10°C; see supporting information S1) suggest that CCS either contained a substantial fraction of very young water recharged only weeks prior to sampling during the spring or the sampled water partially reequilibrated with the atmosphere. The other springs were sampled in October with PF ages 7 to 14 years. Mean T_r and A_e values for the spring samples were 5.5°C and 0.0011 cm^3STP/g , respectively.

Measured concentrations of N_2 and Ar in Copper Creek were very close to computed equilibrium concentrations for the stream water (Table S2 and Figures S2a and S2b), indicating a relatively small τ_g (relatively large v_g) for N_2 and Ar. Because v_g is generally positively correlated with stream gradient (Gleeson et al., 2018), a relatively large v_g is consistent with Copper Creek's steep gradient of ~0.09 above the sample location. In contrast, measured concentrations of SF_6 and CFC-113 were below equilibrium concentrations for the stream water (Table S2 and Figures S2c and S2d). This suggests that (a) the age of groundwater discharging into the stream was sufficiently large that the difference between C_{gw} and C_e was nontrivial (on the order of years rather than weeks/months) and (b) though τ_g values were relatively small for Copper Creek, they were still large enough so that the age tracer C_{gw} signal was maintained in the stream. Therefore, despite Copper Creek's high gradient, v_g for the age tracer gases were sufficiently slow to permit application of the method proposed by Sanford et al. (2015). Although SF_6 and CFC-113 were generally well mixed in the atmosphere, local atmospheric concentrations on the day of sampling could be slightly below the Northern Hemisphere 6-month average values used to compute C_e (USGS, 2017), such that C_s was actually equal to C_e to invalidate the method. A comparison of the atmospheric concentrations required to produce the observed stream concentrations with multiple North American atmospheric monitoring sites indicates that this scenario was unlikely (Figure S1).

The measured gas concentrations in the stream did not provide a unique solution for C_{gw} for either SF_6 or CFC-113, allowing a broad range of possible ages for baseflow (supporting information S1). However, the range of allowable age tracer C_{gw} values was well constrained on the high end because atmospheric concentrations of these age tracers have generally increased since their introduction in the middle twentieth century. This high-end constraint on C_{gw} can potentially provide a reliable minimum age constraint for baseflow. Note that allowable CFC-113 C_{gw} values were sufficiently low to indicate recharge predominantly before the mid-1990s when atmospheric concentrations started decreasing. The CFC-113 concentrations

were discarded from the analysis because, for a given value of τ_w , the estimated CFC-113 C_{gw} consistently produced a substantially older mean age (generally by >10 years) than produced by the simultaneously estimated SF_6 C_{gw} regardless of the assumed form of the travel time distribution. This age discrepancy was likely due to either SF_6 contamination from terrigenous production in the subsurface (e.g., Friedrich et al., 2013), CFC-113 degradation occurring under low-oxygen conditions in parts of the aquifer (e.g., Bockgard et al., 2004), or both. A similar discrepancy was observed by Sanford et al. (2015) at some sites in northern Virginia, USA, and they attributed this to terrigenous SF_6 contributions based on evidence of terrigenous SF_6 in groundwater samples from local springs and wells in which concentrations reflected impossibly high atmospheric concentrations. For the Copper Creek samples, we believe that CFC-113 degradation is a more likely explanation because the spring samples in the East River displayed no clear evidence of terrigenous SF_6 contributions. Furthermore, the range of allowable CFC-113 PF and exponential mean ages for baseflow (>30 years) was substantially older than most reported groundwater ages for other mountain watersheds underlain by predominantly crystalline rock (generally <20 years; Manning, 2009; Manning et al., 2019; Plummer et al., 2001; Visser et al., 2019). As such, using the SF_6 measurements to determine a maximum C_{gw} and minimum baseflow age was assumed a more appropriate and conservative approach because any terrigenous additions would increase the estimated C_{gw} , whereas CFC-113 degradation would decrease the estimated C_{gw} .

The maximum SF_6 C_{gw} was estimated through a series of best fit model solutions in which CFC-113 was excluded. A range of SF_6 C_{gw} values were specified, and resulting model fits were evaluated (Table 2 and Figure 2a). Model fits to observed stream water SF_6 concentrations, defined by the sum χ^2 metric, were similar and acceptable ($p > 0.1$) for SF_6 C_{gw} values up to 2.2 fmol/L. For $C_{gw} > 2.3$ fmol/L, model fits declined rapidly and became unacceptable. For the purposes of numerical modeling, we moved forward with the requirement that any flow model-generated baseflow age distribution must produce an SF_6 C_{gw} concentration <2.3 fmol/L to be consistent with the stream age tracer measurements. As noted, in section 3.1.2, values of T_r and A_e must be defined to compute C_{gw} for a given age distribution. Since C_s and C_e were essentially equal for N_2 and Ar, the stream N_2 and Ar concentrations provided no meaningful constraints on T_r and A_e (Figure S3). Therefore, the mean T_r and A_e values derived from the spring samples were assumed in the computation of C_{gw} for the flow model-generated age distributions (see supporting information S1 for additional discussion).

4.2. Integrated Hydrologic Model

4.2.1. Baseflow Age Calibration

Simulated streamflow and the fraction of streamflow that is interflow for a range of historically variable water years are provided in Figure S6. Interflow dominates stream water source during snow melt (April–July) and can be bolstered in the summer and fall by monsoon rains. Interflow fractional contributions to Copper Creek in late August 2017 during the gas tracer experiment are 22% and align with the same fraction of interflow in the median water year (1998) and a dry water year with near-normal monsoon rains (2012). Figure 3 shows the resulting baseflow age distribution at the sampling location CC03 using the originally published flow model. Median baseflow age is 1.5 years, and water table elevations are shallow with 64% of recharged water moving through the top model layer which is alluvium (<8 m). Figure 4a illustrates the hyperlocalized, topographically controlled and very young groundwater flow paths above the sampling location where granodiorite is the dominant bedrock. Using a Weibull distribution fit to the GSFLOW baseflow age output ($k = 0.28$, $n = 0.44$), the SF_6 groundwater concentration is calculated at 2.74 fmol/L and the sum χ^2 is 147 indicating a statistically insignificant replication of SF_6 stream concentrations (Figure 2).

Geologic parameter adjustments based on a sensitivity analysis (refer to supporting information S2 Figures S6 and S7) to promote older baseflow, with the goal of lowering estimated SF_6 groundwater concentrations, include increasing the granodiorite surface hydraulic conductivity fourfold over the original value of 1.16×10^{-7} to 4.66×10^{-7} m/s and lowering the ratio of horizontal to vertical hydraulic conductivity, or VKA, from 10 to 3. Accompanying changes in bedrock properties was a slight increase in soil storage to replicate observed stream discharge (Nash Sutcliffe Efficiency Log discharge = 0.78). Bedrock reparameterization lowers predicted water table elevations (median depth of groundwater flow equal to 112 m), reduces groundwater flow through the alluvium from 64% to 22% (Figure 3b), and produces a baseflow age distribution (Weibull $k = 0.79$, $n = 0.66$, Figure 3a) capable of reproducing groundwater SF_6 concentration of

Table 2
Selected Model Solutions for Stream Dissolved Gas Concentrations

Modeled gases	Estimated parameters									χ^2 sum (–)	$p = 0.01 \chi^2$ sum (–)	Acceptable fit?
	EA (cm ³ STP/g)	C _{xn} mg/L	T _r (oC)	t _w (hr)	t _{gnar} (hr)	t _{gsf6} (hr)	t _{g113} (hr)	SF ₆ C _{gw} (fmol/L)	CFC-113 C _{gw} (pmol/L)			
N ₂ , Ar	<u>0.000</u>	<u>0.0</u>	<u>10.0</u>	10.7	0.07	—	—	—	—	12.6	24.8	Yes
N ₂ , Ar	<u>0.010</u>	<u>0.0</u>	<u>0.0</u>	14.1	0.08	—	—	—	—	10.6	24.8	Yes
SF ₆ , CFC-113	—	—	—	0.83	—	0.06	0.08	1.32	0.228	19.1	27.2	Yes
SF ₆ , CFC-113	—	—	—	<u>0.50</u>	—	0.06	0.07	1.89	0.267	21.9	27.2	Yes
SF ₆ , CFC-113	—	—	—	<u>1.50</u>	—	0.07	0.14	0.58	0.218	20.7	27.2	Yes
SF ₆ , CFC-113	—	—	—	<u>4.00</u>	—	0.31	0.14	1.35	0.000	24.9	27.2	Yes
SF ₆	—	—	—	0.61	—	0.25	—	<u>2.66</u>	—	100.4	14.7	No
SF ₆	—	—	—	0.91	—	0.37	—	<u>2.60</u>	—	71.8	14.7	No
SF ₆	—	—	—	1.31	—	0.46	—	<u>2.50</u>	—	42.1	14.7	No
SF ₆	—	—	—	1.69	—	0.48	—	<u>2.40</u>	—	26.5	14.7	No
SF ₆	—	—	—	2.07	—	0.49	—	<u>2.30</u>	—	17.9	14.7	No
SF ₆	—	—	—	2.44	—	0.48	—	<u>2.20</u>	—	12.9	14.7	Yes
SF ₆	—	—	—	2.80	—	0.47	—	<u>2.10</u>	—	9.8	14.7	Yes
SF ₆	—	—	—	3.15	—	0.46	—	<u>2.00</u>	—	7.8	14.7	Yes
SF ₆	—	—	—	4.84	—	0.43	—	<u>1.50</u>	—	4.0	14.7	Yes
SF ₆	—	—	—	6.47	—	0.41	—	<u>1.00</u>	—	3.2	14.7	Yes
SF ₆	—	—	—	8.08	—	0.40	—	<u>0.50</u>	—	3.0	14.7	Yes
SF ₆	—	—	—	9.68	—	0.39	—	<u>0.00</u>	—	2.9	14.7	Yes

Note. See text for definitions of model parameters; cm³STP/g = cubic centimeters at standard temperature and pressure per gram of water; underlined parameter values were specified not estimated; — = not estimated or computed; NA = not applicable.

2.2 fmol/L to statistically replicate SF₆ stream water concentrations (sum $\chi^2 = 12.9$, Figure 2). The hydrologic model produces a median baseflow age at CC03 of 7.5 years, which falls within the range of October ages for perennial springs. Figure 4b shows older flow path are now generated in the upper portions of Copper Creek.

4.2.2. Baseflow Age Sensitivity

Using the calibrated model to assess a variety of historical water years indicates that groundwater age contributions are relatively stable 11.8 ± 0.7 years, while late summer baseflow ages range between 3 and 12 years as a function of contributing interflow (Table 3 and Figure S7). A sensitivity analysis perturbing long-term climate from its median condition by incremental changes in the historical median water year daily precipitation shows that groundwater age distributions shift progressively toward older water with

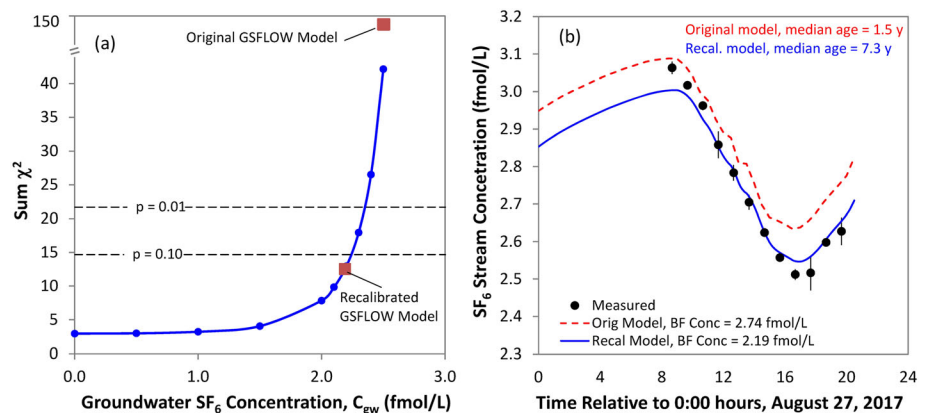


Figure 2. Sampling location CC03 (a) sum χ^2 between predicted and observed stream water concatenations as a function of contribution groundwater SF₆ concentration. Hydrological model (GSFLOW) age estimates are indicated. (b) SF₆ observed water column concentrations with best fit predicted water column concentrations using baseflow age distributions from original GSFLOW and recalibrated GSFLOW simulation.

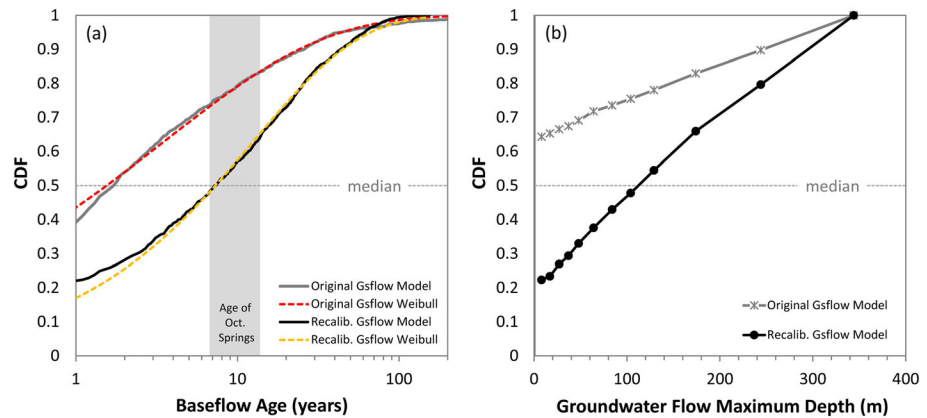


Figure 3. (a) The hydrological model (GSFLOW) recharge weighted baseflow age cumulative distribution (CDF) for late August 2017 at the sampling site CC03 and best fit Weibull distributions to calculate stream water SF₆ concentrations shown in Figure 2b. Age range of springs based on gas data collected in October 2017. Weibull parameters (refer to Equation 3) for the original GSFLOW model $k = 0.28$, $n = 0.44$ and for the recalibrated GSFLOW model $k = 0.08$, $n = 0.66$. (b) CDF of simulated recharge-weighted maximum depth of groundwater flow at the watershed outlet. Symbols placed at average depth of model layers 1 to 12.

decreased precipitation (Figure S11). Warming by +4°C decreases groundwater ages slightly for very wet conditions. Warming during a drought (e.g., 0.8P) removes relatively younger water, while warming during a more intensive drought (e.g., 0.4P) affects all flow paths and the entire distribution shifts older. Warming the basin until snow is converted to rain (+10°C) increases groundwater ages for all conditions, but increases are most dramatic under a drier climate. Removing the forest from Copper Creek increases recharge and shifts groundwater toward younger ages with decreased ages most notable for dry conditions. The median groundwater ages from all scenarios increase with decreasing precipitation and collapse about a single exponential function defined by average annual net recharge, with net recharge defined as recharge minus groundwater ET (Figure 5). Steady-state historical simulations capture spatial and temporal variability of climate variables experienced in the basin over the last 32 years. Resulting median groundwater ages fall within the range of simplistic scenarios developed from water year 1998. Historic conditions similarly plot along the net recharge exponential function. Assuming spatially uniform climate effectively decreases net recharge for the same amount of annual precipitation. The resulting increase in median age is similar to decreasing precipitation by 20% using the spatially distributed climate inputs.

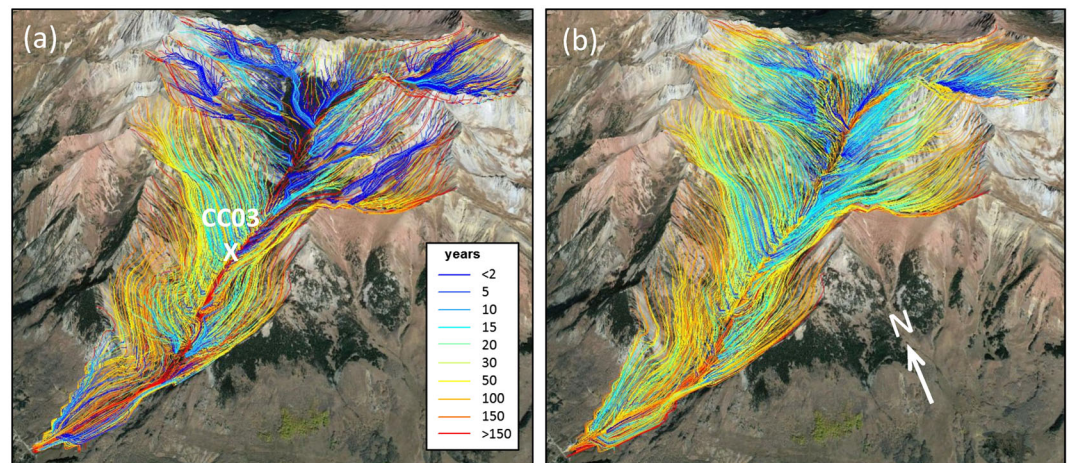


Figure 4. Groundwater flow path ages through the saturated subsurface for (a) the original GSFLOW model and (b) the recalibrated GSFLOW model. The sampling location for the gas tracer experiment (CC03) identified.

Table 3
Simulated Median Ages for Groundwater and Baseflow in Copper Creek, Colorado, for Historical Climate Conditions

Water year	Late Aug. interflow (fraction)	Median age (years)		Climate condition
		Groundwater only	Baseflow ^a	
1998	0.19	11.66	7.80	Median water year
2002	0.03	11.51	11.41	Multiple-year drought 2000–2002
2012	0.20	11.89	7.62	Single large drought after wet year, good monsoon
2017	0.22	12.17	7.48	Wet year, gas tracer experiment
2018	0.01	12.11	11.91	Single large drought after wet year, poor monsoon

^aIncludes interflow.

5. Discussion

Stream water source in the late summer is composed of both shallow ephemeral flow through the soil and saturated groundwater flow through alluvial and bedrock units. Deeper groundwater flow through unweathered bedrock is often treated as negligible in catchment studies (Kirchner, 2009). However, there is a growing awareness that deeper groundwater flow may be an important component in mountain hydrology (Gabrielli et al., 2012; Hale & McDonnell, 2016), and there is a general call to include the bottom of the groundwater system in conceptual models (Brantley et al., 2007; Brooks et al., 2015; Manning & Caine, 2007). However, a fundamental challenge in hydrology is how to define the bottom of the watershed and assess its importance (Condon et al., 2020). The challenge is amplified in steep, snow-dominated, mountain watersheds. These watersheds provide 60–90% of the freshwater world wide (Viviroli & Weingartner, 2008) and are especially vulnerable to climate change (IPCC, 2019). Data describing bedrock properties and deep subsurface flow are scarce in these systems, and little is known how projected warming or reduced snowpack will affect bedrock flow paths and associated streamflow response.

5.1. Age of Baseflow and Depth of Active Groundwater Flow

To help constrain groundwater flow paths in a mountain watershed, we present a novel approach that combines a sophisticated numerical hydrologic model and a new method for dating baseflow using dissolved N_2 , Ar, CFC-113, and SF_6 . The gas tracer experimental procedure is relatively convenient and cost effective as it takes a single day to perform and does not require expensive drilling. Drilling is often impossible in mountainous watersheds due to logistical challenges related to steep topography, deep snowpack, and (in our case) wilderness designation. The stream tracer experiment was not designed for high-gradient rivers with fast gas

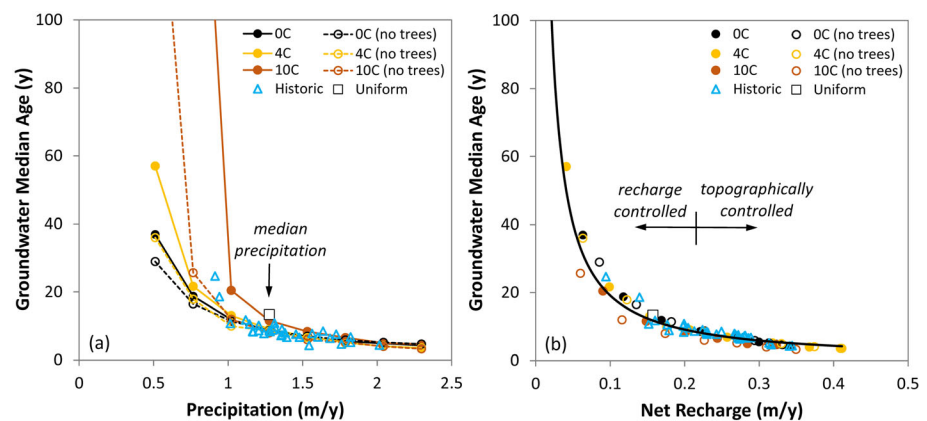


Figure 5. Sensitivity of groundwater median age to drying, warming and forest removal scenarios with respect to (a) precipitation and (b) basin-wide net recharge. The historical median water year precipitation = 1.28 m/year and corresponding quasi-steady-state net recharge (0.22 m/year) separate recharge and topographically controlled groundwater flow paths.

exchange velocities to the atmosphere, and its use in Copper Creek is, in of itself, a methodological question on its effectiveness in alpine environments. Because of fast gas exchange velocities, the approach could not provide a unique baseflow age determination in Copper Creek. However, it did provide a relatively robust upper limit on the groundwater SF₆ concentration and an indirect method for assessing the minimum subsurface travel time in the basin.

The originally published GSFLOW model generates shallow groundwater flow moving predominantly through the alluvium situated on much less conductive bedrock. For late summer conditions in 2017, when the tracer experiment was conducted, baseflow median age is estimated very young at 1.5 years. This produces a statistically insignificant replication of observed SF₆ stream water concentrations. To match stream water SF₆ concentrations, it is necessary to deepen groundwater flow through the upper portions of Copper Creek. Deeper flows increase the age of groundwater (12.2 years) and, with inclusion of interflow, produce a baseflow median age of 7.5 years. In addition to reproducing observed SF₆ stream concentrations, the median age is consistent with PF ages in perennial spring samples collected in October 2017 (10.2 ± 3.4 years). Earlier studies on tranist time modeling in mountainous catchments have tended toward younger ages of 1–5 years (see review by McGuire & McDonnell, 2006) with estimated travel time distributions reliant upon stable isotopes. Yet these tracers cannot inform transport times longer than 4 years, and their exclusive use can bias age distributions and understanding of how catchments store and transmit water (Stewart et al., 2010). Techniques for establishing longer travel times include use of tracers sensitive to older waters (e.g., ³H, CFCs, and SF₆), and a growing number of recent studies suggest that baseflow mean ages in headwater streams may be older than previously thought (>10 years) (Cartwright et al., 2018, 2020). For example, ³H/³He groundwater ages from 17 streamside piezometers along a 3.5-km reach of Handcart Gulch in the Colorado Front Range were all between 8.9 and 19.1 years (Manning et al., 2019). The updated Copper Creek hydrologic model follows this trend in acknowledging older groundwater contributions in mountainous watersheds.

Reconceptualization of the Copper Creek groundwater flow system to produce older water discharged to the stream was largely accomplished by increasing the hydraulic conductivity of the dominant bedrock (granodiorite). This lowered water table elevations and forced more groundwater to travel deeper through the subsurface. We did not explore variations in the hydraulic conductivity depth decay coefficient even though the development of local versus regional groundwater flow patterns is sensitive to this term. Instead, we maintained an average decay coefficient (Jiang et al., 2009) and adjusted the surface conductivity value to limit the solution space. One can speculate that high-relief watersheds like Copper Creek contain older than expected stream flow related to greater permeability and porosity at greater depths due to more intense recent uplift and tectonism associated with mountain building (Jasechko et al., 2016). Final surface permeability for the granodiorite (4.6×10^{-7} m/s) falls within the typical range of 10^{-8} to 10^{-6} m/s for zones of active flow in fractured crystalline bedrock in mountain settings (Katsura et al., 2009; Welch & Allen, 2014). The recalibrated model lowers water table depths such that only 22% of recharged water moves through the alluvium and produces a median depth of groundwaterflow equal to 112 m, with 30% of recharged water reaching depths greater than 200 m. This is somewhat deeper than the maximum depth of active groundwater circulation in crystalline rocks of 100–200 m based on a limited number of prior studies (Markovich et al., 2019; Welch & Allen, 2014). However, Frisbee et al. (2017) estimated active circulation upward to 1,000 m in the crystalline metamorphic rocks of the Sangre de Cristo Mountains, New Mexico. Active circulation depths are a function of tectonic history, lithology, structure, and climate (weathering), and characteristic active flow depths for different bedrock geologic conditions in mountain settings remains largely unknown (Markovich et al., 2019).

We acknowledge that subsurface routing is inherently nonunique in groundwater modeling, and the use of a single hydraulic conductivity value for a given depth for each hydrostratigraphic unit is simplistic and likely overestimates deep flow paths along the highest elevations in Copper Creek in response to low water table elevations. Fractured rock effective porosity is also highly uncertain and complicated by diffusive exchange between mobile water in the fractures and immobile water in the matrix. Effective porosity for age estimates is likely between matrix and fracture porosity. Fractured porosity in unweathered crystalline rocks <1% is common (Tullborg & Larson, 2006), and based on an 80-m borehole drill core within contact-metamorphosed interbedded shale and sandstone in a proximal basin to the East River, we have observed a matrix porosity of 1–10%, centering around 3%. For comparison, modeled effective porosity

of the granodiorite in Copper Creek is equal to 2.5% (depth ≤ 18 m) and 1.25% (depth > 18 m) and deemed appropriate. In light of uncertainties in hydraulic conductivity and porosity, we emphasize that our model is constrained using the minimum tracer-based age for baseflow, and solutions containing older baseflow ages associated with deeper groundwater flow and storage remain entirely plausible for Copper Creek. The current rendition of the Copper Creek hydrologic model suggests that 10% of groundwater is > 50 years. However, these ages are beyond the ability of SF_6 to estimate. Future work would benefit by incorporating tracers such as ^{39}Ar and ^{14}C to better constrain older groundwater (IAEA, 2013).

5.2. Controls on Baseflow Age

The physical reality of mountainous watersheds is that heterogeneities in the system in combination with spatio-variable water inputs create highly diverse flow paths through the basin. As a result, the age distribution of stream water is not time invariant but responds dynamically as the nature of overland flow and hydrologic connectivity change and flow paths and velocities vary with water storage (Botter et al., 2011; Engdahl et al., 2016; Van Der Velde et al., 2012). Transient analysis of individual water years spans the full range of historical climate conditions and associated variability in predicted late summer baseflow median age (3–12 years). The range in baseflow age is due to simulated interflow which is tightly coupled to interannual climate variability with deep and persistent snowpack and/or a wet summer monsoon driving younger baseflow. Our results agree with other studies showing the mobilization and mixing of younger shallow water with older water following wet periods (Howcroft et al., 2018; Hrachowitz et al., 2013). Specifically, Copper Creek baseflow ages align with recent work in Providence Creek, a granodiorite headwater basin in the southern Sierra Nevada mountains of California, with stream ages ranging from 3.3 to 10.3 years with wetter years releasing younger water, as determined using ranked storage functions constrained by radioactive isotopes (Visser et al., 2019). Our results are also consistent with spring mean ages in Sagehen, California, with ages varying from 3–7 years and controlled by the magnitude of the new fraction (< 1 year) that correlated positively to annual maximum snow water equivalent (Manning et al., 2012). Neither of these two studies included tracers capable of dating premodern water (recharged before 1950), meaning that, as with our study, reported ages and interannual age variations could be greater. However, Manning et al. (2012) reported that most samples contained little premodern water based on multiyear comparisons between different tracers.

In contrast to variable baseflow age controlled by interflow contributions, Copper Creek simulated groundwater flow paths and associated ages showed low variance about the mean (11.8 years) deviating by only 0.7 years despite drastically different snow accumulation and stream dynamics for the years assessed. Interannual stability in groundwater flow represents a basin in equilibrium with its historical climate and watershed structure (i.e., topography, land use, and geology). Topographic controls have also long been recognized as controlling local, intermediate, and regional groundwater flow systems (Toth, 1963; Winter et al., 2001) and have been identified as the single most important control on catchment-scale transport (McGuire et al., 2005). Additionally, the influence of precipitation magnitude and type (Carroll et al., 2017), vegetation (Rukundo & Doğan, 2019), bedrock lithology (Onda et al., 2006), and subsurface connectivity (Tetzlaff et al., 2009) have been found to influence recharge and subsequent groundwater flow to streams. The spatial distribution of water inputs may also matter. Recharge in mountain watersheds preferentially occurs in the upper subalpine as a function of large and persistent snowpack (Broxton et al., 2015; Musselman et al., 2008). Badger et al. (2019) using a distributed hydrologic model and remotely sensed estimates of snowpack found more uniform snow distributions melted out 5 weeks earlier and produced up to 9.5% less stream flow than allowing for spatial variability in snowpack. Likewise, we show that assigning a uniform distribution of climate variables effectively reduced recharge to produce older groundwater ages more closely aligned to a basin with 20% less precipitation. In contrast, the sensitivity of median groundwater age to different timings of climate inputs, based on historical variability, is not large. Instead, computed median ages track those determined by the timing of 1998 inputs and scaling the precipitation volume up/down. The exception was during the exceptionally dry years of 2012 and 2018. These years had temperature anomalies of 1.3°C and 2.1°C , respectively, but median ages are larger than the precipitation-scaled 1998 given $+4^\circ\text{C}$. This suggests that under water-limited conditions, the timing of climate variables becomes an important control on groundwater flow paths and residence time.

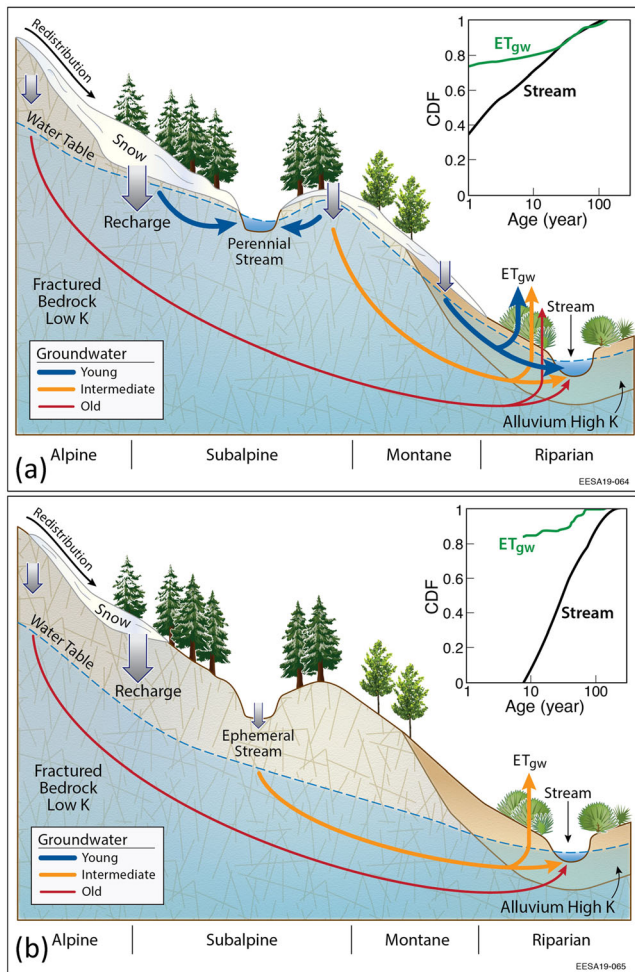


Figure 6. Conceptual model of groundwater flow: (a) topographically controlled flow with a high recharge to hydraulic conductivity ratio (R/K). Baseflow median age insensitive to surface dynamics controlling net recharge. (b) Recharge-controlled groundwater flow with a low R/K . ET_{gw} = groundwater ET.

Forest removal has the potential to increase recharge (and streamflow) by decreasing interception and tree water use, but the effect is muted by corresponding increases in soil evaporation and snowpack sublimation (Biederman et al., 2014; Pugh & Small, 2012). Literature suggests at least a 20% reduction in tree stand is needed to detect a change in water export (Brown et al., 2005; Stednick, 1996), and as such, we removed all the forest as an extreme case. Results indicate that total tree removal changes the timing and quantities of Copper Creek's water balance (Figure S10) but for wetter conditions does not drastically alter groundwater recharge values nor the median groundwater age. Only when the basin is simulated as very dry does increased recharge reduce subsurface residence times with the effect more prominent with warming.

The influence of basin structure on groundwater flow paths is highlighted in Figure 5b, in which travel times collapse toward a single exponential function across a range in simulated recharge conditions. Given the relative insensitivity of vegetation changes to shift the shape and position of the exponential function, it is hypothesized that basin groundwater storage is responsible for travel time sensitivity to recharge. Storage is determined largely by permeability (i.e., lithology) and the ratio of circulation depth to topographic length scale. For example, three-dimensional numerical models have provided guiding principles on recharge controlled versus topographically controlled groundwater systems that in turn drive the length scale of flow paths and associated ages in mountain systems (Gleeson & Manning, 2008; Markovich et al., 2019). To illustrate, Figure 6 depicts the conceptual model of flow path end-members dictated by the ratio of net recharge to hydraulic conductivity (R/K). High R/K produces higher water table elevations and increases the influence of topographically controlled, local flow paths on streamflow generation. If water table elevations are high enough to support perennial streams, then the system is likely permeability limited such that increases in recharge have little effect on changing groundwater flow paths and the median age of groundwater is stable. Conversely, watersheds with lower R/K have deeper water table elevations controlled mainly by the recharge rate. Under these conditions, ephemeral streams emerge, flow paths are less constrained by local topography, and groundwater flow conditions become increasingly sensitive to changes in recharge.

The original Copper Creek model established a very high R/K in the upper portions of the basin to produce a permeability-limited groundwater flow system with shallow water table elevations in which baseflow ages are buffered from possible decreases in recharge. With model reevaluation, the R/K ratio in Copper Creek is lowered. The water table is still topographically controlled, but the newly calibrated model suggests that Copper Creek is much closer to the recharge controlled condition in which groundwater flow paths deepen and groundwater ages increase with relatively small reductions in precipitation. The larger the deviation from the historical median precipitation toward a drier state, the greater the sensitivity of groundwater age is to either recharge decreases (warming) or increases (forest removal). Ameli et al. (2018), using a combination of tritium tracer and a semianalytical flow and transport model in a New Zealand headwater basin, also found groundwater flow paths that lengthen and water ages contributing to streams increase indirectly to recharge rate. This rain-dominated, New Zealand, catchment underlain by early Pleistocene conglomerate reflects a recharged controlled basin that was not readily apparent in Copper Creek without use of the gas tracer observations. Our results suggest that characterization of the bedrock groundwater flow system is fundamentally important to establishing R/K and determining where a basin resides on the topographic and recharge controlled continuum in order to better quantify how groundwater flow may respond to changing climate and land use.

6. Conclusions

There is growing awareness that deeper parts of bedrock aquifers in steep, mountain watersheds could be an important part of a watershed's hydrologic system by storing and transmitting larger amounts of water and having a greater influence on stream source than previously indicated. However, deeper parts of mountain aquifers are very difficult to characterize and information on hydraulic conductivity, porosity, and flow rates at depth remain scarce and the true importance of deeper groundwater flow across different geologic settings remains largely unknown. This knowledge gap is a major impediment to our ability to predict how surface water flow may respond to changes in precipitation, temperature, or land use. Here we present a proof-of-concept for a new and efficient approach for characterizing deeper groundwater flow in a mountain watershed using stream water concentrations of N₂, Ar, CFC-113, and SF₆. While interflow produces considerable variability in baseflow age as a function of interannual variability in climate, the deeper groundwater flow component of baseflow was found more stable (age~12 years). Using gas tracer observations in streamflow, we provide solid evidence of nontrivial groundwater flow to streams that occurs at considerable depth in a mountain watershed of the Upper Colorado River underlain by fractured crystalline rock. The implication for the conceptual model of groundwater flow in this mountain watershed is substantial. Using age tracers to inform an integrated hydrologic model, we move Copper Creek from a topographically controlled basin with groundwater flow paths (age) insensitive to changes in precipitation (and recharge) toward a boarderline recharge controlled groundwater basin in which groundwater flow paths are sensitive to increased aridity. This study clarifies, through a case example, the importance of characterizing the bedrock groundwater system in mountain watersheds to determine where it resides on the R/K spectrum to better predict how groundwater and surface water interactions in steep, mountain basins may respond to future changes in climate or land use.

Data Availability Statement

Data and finite difference model approximations of Equation 1 are available to the public on the U.S. DOE Environmental Systems Science Data Infrastructure for Virtual Ecosystem (<https://data.ess-dive.lbl.gov/view/doi:10.21952/WTR/1572196>). Any use of trade products or firm names is for descriptive purposes only and does not imply endorsement by the U.S. Government.

Acknowledgments

Work was supported by the U.S. Geological Survey 104(g) Grant/Cooperative Agreement G16AP00196 and the U.S. Department of Energy Office of Science under contract DE-AC02-05CH11231 as part of Lawrence Berkeley National Laboratory Watershed Function Science Focus Area. Funding from the U.S. Geological Survey Mineral Resources Program funded Dr. Manning's time. Additional funding through NSF ROA Award 1624073 helped fund Dr. Marchetti. We wish to thank Ward Sanford with the USGS for sharing his baseflow age model template for gas tracer processing and Jerry Casile with the U.S. Geological Survey Reston Groundwater Dating Laboratory for his time and expertise on analytical processing of water samples for dissolved gases. We acknowledge the WCU Bartleson-Prather Research Fund for funding WCU undergraduate Manya Ruckhaus who aided in Copper Creek stream and perennial spring sampling. Lastly, we would like to express appreciation to the Rocky Mountain Biological Laboratory for handling U.S. Forest Service permitting in the Maroon Bells Wilderness. We appreciate the time and valuable comments from Ward Sanford, Ian Cartwright, and four unanimous reviewers.

References

- Aeschbach-Hertig, W., Peeters, F., Beyerle, U., & Kipfer, R. (2000). Paleotemperature reconstruction from noble gases in ground water taking into account equilibration with entrapped air. *Nature*, *405*(6790), 1040–1044. <https://doi.org/10.1038/35016542>
- Allen, R. G., Trezza, R., Kilic, A., Tasumi, M., & Li, H. (2013). Sensitivity of Landsat-scale energy balance to aerodynamic variability in mountains and complex terrain. *Journal of the American Water Resources Association*, *49*(3), 592–604. <https://doi.org/10.1111/jawr.12055>
- Ameli, A. A., Gabrielli, C., Morgenstern, U., & McDonnell, J. J. (2018). Groundwater subsidy from headwaters to their parent water watershed: A combined field-modeling approach. *Water Resources Research*, *54*, 5110–5125. <https://doi.org/10.1029/2017WR022356>
- Badger, A. M., Livneh, B., & Molotch, N. P. (2019). 'On the role of spatial snow distribution on Alpine catchment hydrology', *World Environmental and Water Resources Congress*, pp. 215–225.
- Biederman, J. A., Harpold, A. A., Gochis, D. J., Ewers, B. E., Reed, D. E., Papuga, S. A., & Brooks, P. D. (2014). Increased evaporation following widespread tree mortality limits streamflow response. *Water Resources Research*, *50*, 5395–5409. <https://doi.org/10.1002/2013WR014994>
- Bockgard, N., Rodhe, A., & Olsson, K. A. (2004). Accuracy of CFC groundwater dating in a crystalline bedrock aquifer: Data from a site in southern Sweden. *Hydrogeology Journal*, *12*, 171–183.
- Botter, G., Bertuzzo, E., & Rinaldo, A. (2011). Catchment residence and travel time distributions: The master equation. *Geophysical Research Letters*, *38*, L11403. <https://doi.org/10.1029/2011GL047666>
- Brantley, S. L., Goldhaber, M. B., & Ragnarsdottir, K. V. (2007). Crossing disciplines and scales to understand the critical zone. *Elements*, *3*(5), 307–314. <https://doi.org/10.2113/gselements.3.5.307>
- Brooks, P. D., Chorover, J., Fan, Y., Godsey, S. E., Maxwell, R. M., McNamara, J. P., & Tague, C. (2015). Hydrological partitioning in the critical zone: Recent advances and opportunities for developing transferable understanding of water cycle dynamics. *Water Resources Research*, *51*, 6973–6987. <https://doi.org/10.1002/2015WR017039>
- Brown, A. E., Zhang, L., McMahon, T. A., Western, A. W., & Vertessy, R. A. (2005). A review of paired catchment studies for determining changes in water yield resulting from alterations in vegetation. *Journal of Hydrology*, *310*(1–4), 28–61. <https://doi.org/10.1016/j.jhydrol.2004.12.010>
- Broxton, P. D., Harpold, A. A., Biederman, J. A., Troch, P. A., Molotch, N. P., & Brooks, P. D. (2015). Quantifying the effects of vegetation structure on snow accumulation and ablation in mixed-conifer forests. *Ecohydrology*, *8*(6), 1073–1094. <https://doi.org/10.1002/eco.1565>
- Busenberg, E., & Plummer, L. N. (2002). Dating young water with sulfur hexafluoride: Natural and anthropogenic sources of sulfur hexafluoride. *Water Resources Research*, *36*(10), 3011–3030. <https://doi.org/10.1029/2000WR900151>

- Carroll, R. W. H., Bearup, L. A., Brown, W., Dong, W., Bill, M., & Williams, K. H. (2018). Factors controlling seasonal groundwater and solute flux from snow-dominated basins. *Hydrological Processes*, *32*(14), 2187–2202. <https://doi.org/10.1002/hyp.13151>
- Carroll, R. W. H., Deems, J. S., Niswonger, R., Schumer, R., & Williams, K. H. (2019). The importance of interflow to groundwater recharge in a snowmelt-dominated headwater basin. *Geophysical Research Letters*, *46*, 5899–5908. <https://doi.org/10.1029/2019GL082447>
- Carroll, R. W. H., Huntington, J. L., Snyder, K. A., Niswonger, R. G., Morton, C., & Stringham, T. K. (2017). Evaluating mountain meadow groundwater response to Pinyon-Juniper and temperature in a great basin watershed. *Ecohydrology*, *10*(1), e1792–e1718. <https://doi.org/10.1002/eco.1792>
- Cartwright, I., Atkinson, A. P., Gilfedder, B. S., Hofmann, H., Cendón, D. I., & Morgenstern, U. (2018). Using geochemistry to understand water sources and transit times in headwater streams of a temperate rainforest. *Applied Geochemistry*, *99*, 1–12. <https://doi.org/10.1016/j.apgeochem.2018.10.018>
- Cartwright, I., Morgenstern, U., & Hofmann, H. (2020). Concentration versus streamflow trends of major ions and tritium in headwater streams as indicators of changing water stores. *Hydrological Processes*, *34*(2), 485–505. <https://doi.org/10.1002/hyp.13600>
- Cesano, D., Bagtzoglou, A. C., & Olofsson, B. (2003). Quantifying fractured rock hydraulic heterogeneity and groundwater inflow prediction in underground excavations: The heterogeneity index. *Tunnelling and Underground Space Technology*, *18*(1), 19–34. [https://doi.org/10.1016/S0886-7798\(02\)00098-6](https://doi.org/10.1016/S0886-7798(02)00098-6)
- Condon, L. E., Markovich, K. H., Kelleher, C. A., McDonnell, J. J., Ferguson, G., & McIntosh, J. C. (2020). Where is the bottom of a watershed? *Water Resources Research*, *56*, e2019WR026010. <https://doi.org/10.1029/2019WR026010>
- Danesh-Yazdi, M., Klaus, J., Condon, L. E., & Maxwell, R. M. (2018). Bridging the gap between numerical solutions of travel time distributions and analytical storage selection functions. *Hydrological Processes*, *32*(8), 1063–1076. <https://doi.org/10.1002/hyp.11481>
- Deems, J. S., Fassnacht, S. R., & Elder, K. J. (2006). Fractal distribution of snow depth from LiDAR data. *Journal of Hydrometeorology*, *7*(2), 285–297. <https://doi.org/10.1175/JHM487.1>
- Engdahl, N. B., McCallum, J. L., & Massoudieh, A. (2016). Transient age distributions in subsurface hydrologic systems. *Journal of Hydrology*. Elsevier B.V., *543*, 88–100. <https://doi.org/10.1016/j.jhydrol.2016.04.066>
- Fang, Z., Carroll, R. W. H., Schumer, R., Harman, C., Wilusz, D., & Williams, K. H. (2019). Streamflow partitioning and transit time distribution in snow-dominated basins as a function of climate. *Journal of Hydrology*. Elsevier, *570*(December 2018), 726–738. <https://doi.org/10.1016/j.jhydrol.2019.01.029>
- Friedrich, R., Vero, G., von Rohden, C., Lessmann, B., Kipfer, R., & Aeschbach-Hertig, W. (2013). Factors controlling terrigenous SF6 in young groundwater of the Odenwald region (Germany). *Applied Geochemistry*, *33*, 318–329. <https://doi.org/10.1016/j.apgeochem.2013.03.002>
- Frisbee, M. D., Tolley, D. G., & Wilson, J. L. (2016). Field estimates of groundwater circulation depths in two mountainous watersheds in the western U.S. and the effect of deep circulation on solute concentrations in streamflow. *Water Resources Research*, *53*, 2693–2715. <https://doi.org/10.1002/2016WR019553>
- Frisbee, M. D., Tolley, D. G., & Wilson, J. L. (2017). Field estimates of groundwater circulation depths in two mountainous watersheds in the western U.S. and the effect of deep circulation on solute concentrations in streamflow. *Water Resources Research*, *53*, 2693–2715. <https://doi.org/10.1002/2016WR019553>
- Gabrielli, C. P., McDonnell, J. J., & Jarvis, W. T. (2012). The role of bedrock groundwater in rainfall-runoff response at hillslope and catchment scales. *Journal of Hydrology*. Elsevier B.V., *450–451*, 117–133. <https://doi.org/10.1016/j.jhydrol.2012.05.023>
- Gaskill, D., Mutschler, F., & Kramer, J. (1991). Geologic map of the Gothic Quadrangle, Gunnison County, Colorado. <https://doi.org/10.3133/gq1689>
- Gleeson, T., & Manning, A. H. (2008). Regional groundwater flow in mountainous terrain: Three-dimensional simulations of topographic and hydrogeologic controls. *Water Resources Research*, *44*, W10403. <https://doi.org/10.1029/2008WR006848>
- Gleeson, T., Manning, A. H., Popp, A., Zane, M., & Clark, J. F. (2018). The suitability of using dissolved gases to determine groundwater discharge to high gradient streams. *Journal of Hydrology*. Elsevier B.V., *557*, 561–572. <https://doi.org/10.1016/j.jhydrol.2017.12.022>
- Gusyeve, M. A., Abrams, D., Toews, M. W., Morgenstern, U., & Stewart, M. K. (2014). A comparison of particle-tracking and solute transport methods for simulation of tritium concentrations and groundwater transit times in river water. *Hydrology and Earth System Sciences*, *18*, 3109–3119. <https://doi.org/10.5194/hess-18-3109-2014>
- Hale, V. C., & McDonnell, J. J. (2016). Effect of bedrock permeability on stream base flow mean transit time scaling relations: 1. A multiscale catchment intercomparison. *Water Resources Research*, *52*, 1358–1374. <https://doi.org/10.1002/2014WR016124>
- Harbaugh, A. W. (2005). 'MODFLOW-2005, the U.S. Geological Survey modular groundwater model—The ground-water flow process', U. S. Geological Survey Technical Methods, Book 6, p. Ch. A16.
- Harman, C. J. (2015). Time-variable transit time distributions and transport: Theory and application to storage-dependent transport of chloride in a watershed. *Water Resources Research*, *51*, 1–30. <https://doi.org/10.1002/2014WR015707>
- Harpold, A., Brooks, P., Rajagopal, S., Heidbüchel, I., Jardine, A., & Stielstra, C. (2012). Changes in snowpack accumulation and ablation in the intermountain west. *Water Resources Research*, *48*, W11501. <https://doi.org/10.1029/2012WR011949>
- Hay, L. E., Markstrom, S. L., & Ward-Garrison, C. D. (2011). Watershed-scale response to climate change through the 21st century for selected basins across the United States. *Earth Interactions*, *15*(17), 1–37. <https://doi.org/10.1175/2010EI370.1>
- Heidbüchel, I., Troch, P. A., Lyon, S. W., & Weiler, M. (2012). The master transit time distribution of variable flow systems. *Water Resources Research*, *48*, W06520. <https://doi.org/10.1029/2011WR011293>
- Howcroft, W., Cartwright, I., & Morgenstern, U. (2018). Mean transit times in headwater catchments: Insights from the Otway Ranges, Australia. *Hydrology and Earth System Sciences*, *22*(1), 635–653. <https://doi.org/10.5194/hess-22-635-2018>
- Hrachowitz, M., Savenije, H., Bogaard, T. A., Tetzlaff, D., & Soulsby, C. (2013). What can flux tracking teach us about water age distribution patterns and their temporal dynamics? *Hydrology and Earth System Sciences*, *17*(2), 533–564. <https://doi.org/10.5194/hess-17-533-2013>
- Hubbard, S. S., Williams, K. H., Agarwal, D., Banfield, J., Beller, H., Bouskill, N., et al. (2018). The East River, Colorado, watershed: A mountainous community testbed for improving predictive understanding of multiscale hydrological–biogeochemical dynamics. *Vadose Zone Journal*, *17*(1), 180061. <https://doi.org/10.2136/vzj2018.03.0061>
- Huntington, J. L., & Niswonger, R. G. (2012). Role of surface-water and groundwater interactions on projected summertime streamflow in snow-dominated regions: An integrated modeling approach. *Water Resources Research*, *48*, W11524. <https://doi.org/10.1029/2012WR012319>
- International Atomic Energy Agency (IAEA) (2013). Isotope methods for dating old groundwater. Vienna, Austria. p. 30. https://www-pub.iaea.org/MTCD/Publications/PDF/Pub1587_web.pdf

- IPCC (2019). *IPCC special report on the ocean and cryosphere in a changing climate*. In H.-O. Pörtner Roberts, et al. (Eds.). Retrieved from <https://www.ipcc.ch/report/srocc/> https://www.ipcc.ch/site/assets/uploads/sites/3/2019/12/SROCC_FullReport_FINAL.pdf
- Jasechko, S., Kirchner, J. W., Welker, J. M., & McDonnell, J. J. (2016). Substantial proportion of global streamflow less than three months old. *Nature Geoscience*, *9*(2), 126–129. <https://doi.org/10.1038/ngeo2636>
- Jiang, X.-W., Wan, L., Wang, X.-S., Ge, S., & Liu, J. (2009). Effect of exponential decay in hydraulic conductivity with depth on regional groundwater flow. *Geophysical Research Letters*, *36*, L24402. <https://doi.org/10.1029/2009GL01251>
- Katsura, S., Kosugi, K. I., Mizutani, T., & Mizuyama, T. (2009). Hydraulic properties of variously weathered granitic bedrock in headwater catchments. *Vadose Zone Journal*, *8*(3), 557–573. <https://doi.org/10.2136/vzj2008.0142>
- Kirchner, J. W. (2009). Catchments as simple dynamical systems: Catchment characterization, rainfall-runoff modeling, and doing hydrology backward. *Water Resources Research*, *45*, W02429. <https://doi.org/10.1029/2008WR006912>
- LANDFIRE (2015). *Existing vegetation type and cover layers, U.S. Department of the Interior, Geological Survey*. Available at: <http://landfire.cr.usgs.gov/viewer/> (accessed May 2017).
- Mahlknecht, J., Hernández-Antonio, A., Eastoe, C. J., Tamez-Meléndez, C., Ledesma-Ruiz, R., Ramos-Leal, J. A., & Ornelas-Soto, N. (2017). Understanding the dynamics and contamination of an urban aquifer system using groundwater age (^{14}C , ^3H , CFCs) and chemistry. *Hydrological Processes*, *31*(13), 2365–2380. <https://doi.org/10.1002/hyp.11182>
- Manning, A. H. (2009). 'Ground-water temperature, noble gas, and carbon isotope data from the Española Basin, New Mexico', *U.S. Geological Survey Scientific Investigations Report*, 2008–5200, p. 69.
- Manning, A. H., & Caine, J. S. (2007). Groundwater noble gas, age, and temperature signatures in an Alpine watershed: Valuable tools in conceptual model development. *Water Resources Research*, *43*, W04404. <https://doi.org/10.1029/2006WR005349>
- Manning, A. H., Clark, J. F., Diaz, S. H., Rademacher, L. K., Earman, S., & Plummer, L. N. (2012). Evolution of groundwater age in a mountain watershed over a period of thirteen years. *Journal of Hydrology*. Elsevier B.V., *460–461*, 13–28. <https://doi.org/10.1016/j.jhydrol.2012.06.030>
- Manning, A. H., Morrison, J. M., Wanty, R. B., & Mills, C. T. (2019). Using stream-side groundwater discharge for geochemical exploration in mountainous terrain. *Journal of Geochemical Exploration*, *209*, 106415. <https://doi.org/10.1016/j.gexplo.2019.106415>
- Markovich, K. H., Manning, A. H., Condon, L. E., & McIntosh, J. C. (2019). Mountain-block recharge: A review of current understanding. *Water Resources Research*, *55*, 8278–8304. <https://doi.org/10.1029/2019WR025676>
- Markstrom, S. L., Niswonger, R. G., Regan, R. S., Prudic, D. E., & Barlow, P. M. (2008). 'GSFLOW—Coupled ground-water and surface-water flow model based on the integration of the precipitation-runoff modeling system (PRMS) and the modular ground-water flow model (MODFLOW-2005)', *U.S. Geological Survey Techniques and Methods*, 6-D1, p. 240.
- Markstrom, S. L., Regan, R. S., Hay, L. E., Viger, R. J., Webb, R. M., Payn, R. A., & LaFontaine, J. H. (2015). 'PRMS-IV, the precipitation-runoff modeling system, version 4', *U.S. Geological Survey Techniques and Methods, book 6, chap. B7*, p. 158. <https://doi.org/10.3133/tm6B7>
- Maxwell, R. M., Condon, L. E., Kollet, S. J., Maher, K., Haggerty, R., & Forrester, M. M. (2016). The imprint of water and geology on residence times in groundwater. *Geophysical Research Letters*, *43*, 701–708. <https://doi.org/10.1002/2015GL066916>
- McGuire, K. J., & McDonnell, J. J. (2006). A review and evaluation of catchment transit time modeling. *Journal of Hydrology*, *330*(3–4), 543–563. <https://doi.org/10.1016/j.jhydrol.2006.04.020>
- McGuire, K. J., McDonnell, J. J., Weiler, M., Kendall, C., McGlynn, B. L., Welker, J. M., & Seibert, J. (2005). The role of topography on catchment-scale water residence time. *Water Resources Research*, *41*, W05002. <https://doi.org/10.1029/2004WR003657>
- Meixner, T., Manning, A. H., Stonestrom, D. A., Allen, D. M., Ajami, H., Blasch, K. W., et al. (2016). Implications of projected climate change for groundwater recharge in the western United States. *Journal of Hydrology*. Elsevier B.V., *534*(January), 124–138. <https://doi.org/10.1016/j.jhydrol.2015.12.027>
- Meyer, J. L., Strayer, D. L., Wallace, J. B., Eggert, S. L., Helfman, G. S., & Leonard, N. E. (2007). The contribution of headwater streams to biodiversity in river networks. *Journal of the American Water Resources Association*, *43*(1), 86–103. <https://doi.org/10.1111/j.1752-1688.2007.00008.x>
- Miller, M. P., Buto, S. G., Susong, D. D., & Rumsey, C. A. (2016). The importance of base flow in sustaining surface water flow in the Upper Colorado River Basin. *Water Resources Research*, *52*, 3547–3562. <https://doi.org/10.1002/2015WR017963>
- Missik, J. E. C., Liu, H., Gao, Z., Huang, M., Chen, X., Arntzen, E., et al. (2019). Groundwater-river water exchange enhances growing season evapotranspiration and carbon uptake in a semiarid riparian ecosystem. *Journal of Geophysical Research: Biogeosciences*, *124*, 99–114. <https://doi.org/10.1029/2018JG004666>
- Musselman, K. N., Molotch, N. P., & Brooks, P. D. (2008). Effects of vegetation on snow accumulation and ablation in a mid-latitude sub-alpine forest. *Hydrological Processes*, *22*(15), 2767–2776. <https://doi.org/10.1002/hyp.7050>
- Niswonger, R. G., Panday, S., & Ibaraki, M. (2011). 'MODFLOW-NWT, A Newton formulation for MODFLOW-2005', *U.S. Geological Survey Groundwater Resources Program, Techniques and Methods*, 6-A37, p. 44.
- Niswonger, R. G., Prudic, D. E., & Regan, R. S. (2006). Documentation of the unsaturated-zone flow (UZf1) package for modeling unsaturated flow between the land surface and the water table with MODFLOW-2005', *U.S. Geological Survey Survey Techniques and Methods*. 6-A19, 62 p.
- NRCS (1991). Web soil survey, United States Department of Agriculture. Available at: <http://websoilsurvey.nrcs.usda.gov/> accessed March 2016.
- Onda, Y., Tsujimura, M., Fujihara, J. I., & Ito, J. (2006). Runoff generation mechanisms in high-relief mountainous watersheds with different underlying geology. *Journal of Hydrology*, *331*(3–4), 659–673. <https://doi.org/10.1016/j.jhydrol.2006.06.009>
- Painter, T. H., Berisford, D. F., Boardman, J. W., Bormann, K. J., Deems, J. S., Gehrke, F., et al. (2016). The airborne snow observatory: Fusion of scanning lidar, imaging spectrometer, and physically-based modeling for mapping snow water equivalent and snow albedo. *Remote Sensing of Environment*. Elsevier Inc, *184*, 139–152. <https://doi.org/10.1016/j.rse.2016.06.018>
- Perdril, J., Brooks, P. D., Swetnam, T., Lohse, K. A., Rasmussen, C., Litvak, M., et al. (2018). A net ecosystem carbon budget for snow dominated forested headwater catchments: Linking water and carbon fluxes to critical zone carbon storage. *Biogeochemistry*, *138*(3), 225–243. <https://doi.org/10.1007/s10533-018-0440-3>
- Plummer, L. N., Busenberg, E., Böhlke, J. K., Nelms, D. L., Michel, R. L., & Schlosser, P. (2001). Groundwater residence times in Shenandoah National Park, Blue Ridge Mountains, Virginia, USA: A multi-tracer approach. *Chemical Geology*, *179*(1–4), 93–111. [https://doi.org/10.1016/S0009-2541\(01\)00317-5](https://doi.org/10.1016/S0009-2541(01)00317-5)
- Pollock, D. W. (2016). 'User guide for MODPATH version 7—A particle-tracking model for MODFLOW', *U.S. Geological Survey Open-File Report*, 2016–1086, p. 35. <https://doi.org/10.3133/ofr20161086>

- Pugh, E., & Small, E. (2012). The impact of pine beetle infestation on snow accumulation and melt in the headwaters of the Colorado River. *Ecohydrology*, 5(4), 467–477. <https://doi.org/10.1002/eco.239>
- Rukundo, E., & Doğan, A. (2019). Dominant influencing factors of groundwater recharge spatial patterns in Ergene river catchment, Turkey. *Water (Switzerland)*, 11(4), 653, 653. <https://doi.org/10.3390/w11040653>
- Rumsey, C. A., Miller, M. P., Susong, D. D., Tillman, F. D., & Anning, D. W. (2015). Regional studies regional scale estimates of baseflow and factors influencing baseflow in the Upper Colorado River Basin. *Journal of Hydrology*. Elsevier B.V., 4, 91–107.
- Sanford, W. E., Casile, G., & Haase, K. B. (2015). Dating base flow in streams using dissolved gases and diurnal temperature changes. *Water Resources Research*, 51, 9790–9803. <https://doi.org/10.1002/2014WR016796>
- Smith, A. A., Tetzlaff, D., & Soulsby, C. (2018). Using StorAge selection functions to quantify ecohydrological controls on the time-variant age of evapotranspiration, soil water, and recharge. *Hydrology and Earth System Sciences Discussions*, (February), 1–25. <https://doi.org/10.5194/hess-2018-57>
- Solomon, D. K., Cook, P. G., & Sanford, W. E. (1998). In C. Kendall & J. McDonnell (Eds.), *Dissolved gases in subsurface hydrology, isotope tracers in catchment hydrology*. Amsterdam: Elsevier. <https://www.sciencedirect.com/science/article/pii/B9780444815460500161>
- Stednick, J. D. (1996). Monitoring the effects of timber harvest on annual water yield. *Journal of Hydrology*, 176(1–4), 79–95. [https://doi.org/10.1016/0022-1694\(95\)02780-7](https://doi.org/10.1016/0022-1694(95)02780-7)
- Stewart, M. K., Mogenstern, U., & McDonnell, J. J. (2010). Truncation of stream residence time: How the use of stable isotopes has skewed our concept of streamwater age and origin. *Hydrological Processes*, 24, 1646–1659. <https://doi.org/10.1002/hyp.7576>
- Stute, M., & Schlosser, P. (2000). Atmospheric noble gases. In P. G. Cook & A. L. Herczeg (Eds.), *Environmental tracers in subsurface hydrology* (pp. 349–377). New York: Springer. https://doi.org/10.1007/978-1-4615-4557-6_11
- Tetzlaff, D., Seibert, J., McGuire, K. J., Laudon, H., Burns, D. A., Dunn, S. M., & Soulsby, C. (2009). How does landscape structure influence catchment scale transit time across different geomorphic provinces? *Hydrological Processes*, 23(6), 945–953. <https://doi.org/10.1002/hyp.7240>
- Toth, J. (1963). A theoretical analysis of groundwater flow in small drainage basins. *Journal of Geophysical Research*, 68, 2354–2356. <https://doi.org/10.1029/JZ068i008p02354>
- Tullborg, E.-L., & Larson, S. A. (2006). ‘Porosity in crystalline rocks—A matter of scale’, *Engineering Geology*, 84(1–2), pp. 75–83. <https://doi.org/10.1016/j.enggeo.2005.12.001>
- USGS (2017). *U.S. Geological Survey Groundwater Age Dating Laboratory*, U.S. Geological Survey, Reston, VA. Available at: <http://water.usgs.gov/lab/> (Accessed: 23 March 2017).
- van der Velde, Y., Torfs, P. J. J. F., van der Zee, S. E. A. T. M., & Uijlenhoet, R. (2012). Quantifying catchment-scale mixing and its effect on time-varying travel time distributions. *Water Resources Research*, 48, W06536. <https://doi.org/10.1029/2011WR011310>
- Visser, A., Thaw, M., Deinhard, A., Bibby, R., Safeeq, M., Conklin, M., et al. (2019). Cosmogenic isotopes unravel the Hydrochronology and water storage dynamics of the southern sierra critical zone. *Water Resources Research*, 55, 1429–1450. <https://doi.org/10.1029/2018WR023665>
- Viviroli, D., & Weingartner, R. (2008). Water towers—A global view of the hydrological importance of mountains. In E. Wiegandt (Ed.), *Mountains: Sources of water, sources of knowledge. Advances in global change research* (Vol. 31, pp. 15–20). Dordrecht: Springer. https://doi.org/10.1007/978-1-4020-6748-8_2
- Wang, K., & Dickinson, R. (2012). A review of global terrestrial evapotranspiration: Observation, modeling, climatology, and climate variability. *Reviews of Geophysics*, 50(2011), 1–54. <https://doi.org/10.1029/2011RG000373>.1.INTRODUCTION
- Welch, L. A., & Allen, D. M. (2014). Caractéristiques de la conductivité hydraulique en région de montagne et implications pour la conceptualisation des écoulements souterraines dans la roche en place. *Hydrogeology Journal*, 22(5), 1003–1026. <https://doi.org/10.1007/s10040-014-1121-5>
- Winnick, M. J., Carroll, R. W. H., Williams, K. H., Maxwell, R. M., Dong, W., & Maher, K. (2017). Snowmelt controls on concentration-discharge relationships and the balance of oxidative and acid-base weathering fluxes in an alpine catchment, East River, Colorado. *Water Resources Research*, 53, 2507–2523. <https://doi.org/10.1002/2016WR019724>
- Winter, T. C., Rosenberry, D. O., & LaBaugh, J. W. (2001). The concept of hydrologic landscapes. *Journal of the American Water Resources Association*, 37, 335–349. <https://doi.org/10.1111/j.1752-1688.2001.tb00973.x>